

⁴Deissler, R. G., "Analysis of Turbulent Heat Transfer, Mass Transfer and Friction in Smooth Tubes at High Prandtl and Schmidt Numbers," NACA Rept. 1210, 1954.

⁵van Driest, E. R., "The Turbulent Boundary Layer with Variable Prandtl Number," North America Aviation, Rept. A1-1914, 1954.

⁶Spalding, D. B., "Heat Transfer to a Turbulent Stream from a Surface with Stepwise Discontinuity in Wall Temperature," *International Developments in Heat Transfer*, Pt. 2, ASME, New York, 1961, pp. 439-446.

⁷Reshotko, E. and Tucker, M., "Approximate Calculation of the Compressible Turbulent Boundary Layer with Heat Transfer and Arbitrary Pressure Gradient," NASA TN 4154, Dec. 1957.

⁸Cohen, C. B., "A Method for Computing Turbulent Heat Transfer in the Presence of a Streamwise Pressure Gradient for Bodies in High Speed Flow," NACA Memo 1-2-59L, 1959.

⁹Tetervin, N., "Approximate Calculation of Reynolds Analogy for Turbulent Boundary Layer with Pressure Gradient," *AIAA Journal*, Vol. 7, June 1969, pp. 1079-1085.

¹⁰Jayatillaka, C. L. V., "The Influence of Prandtl Number and Surface Roughness on the Resistance of the Laminar Sublayer to Momentum and Heat Transfer," *Progress in Heat and Mass Transfer*, 1st ed., edited by U. Grigull and E. Hahne, Pergamon Press, New York, 1969, p. 1.

¹¹Kline, S. J., Cockrell, D. J., Morkovin, M. V., and Sovaran, G., "Computed Turbulent Boundary Layers, Vol. 1," Dept. of Mechanical Engineering, Stanford University, Stanford, Calif., AFOSR-IFP-Stanford, 1968.

¹²Sasman, P. K. and Cresci, R. J., "Compressible Turbulent Boundary Layer with Pressure Gradient and Heat Transfer," *AIAA Journal*, Vol. 4, Jan. 1966, pp. 19-25.

¹³Nakayama, A. and Chow, W. L., "Calculation of Transonic Boattail Flow at a Small Angle of Attack," Dept. of Mechanical and Industrial Engineering, University of Illinois, Urbana-Champaign, Rept. ME-TN-395-6, prepared for NASA Research Grant NGL 14-005-140, 1979.

¹⁴Rubesin, M. W. and Inouye, M., "Forced Convection, External Flow," *Handbook of Heat Transfer*, edited by Rohsenow and Hartnett, McGraw-Hill Book Co., New York, 1973, pp. 8-148.

Explicit Representations of the Complete Velocity Profile in a Turbulent Boundary Layer

A. Liakopoulos*

University of Florida, Gainesville, Florida

Nomenclature

B	= constant in the logarithmic law
$e(y^+)$	= difference of the approximation, Eq. (10)
$f(y^+)$	= function representing the law of the wall
g	= function representing the law of the wake
Re_θ	= Reynolds number based on momentum thickness
u	= mean velocity component parallel to the wall
u_e	= mean velocity at the boundary-layer edge
u_τ	= friction velocity, $(\tau_w/\rho)^{1/2}$
u^+	= dimensionless u velocity, u/u_τ
w	= wake function
y	= coordinate normal to the wall
y^+	= dimensionless distance from the wall, yu_τ/ν
δ, δ^*, θ	= boundary-layer, displacement, and momentum thickness, respectively
κ	= von Kármán constant
ν	= molecular kinematic viscosity
Π	= Coles wake parameter

ρ = fluid density
 τ_w = wall shear stress

Introduction

It is well known that most of the commonly used turbulence models lead to parabolic systems when coupled with the boundary-layer equations. Consequently, starting a differential method of predicting turbulent boundary layers requires the specification of initial profiles for the dependent variables. For this purpose, an accurate and computationally convenient expression for the mean velocity distribution is of particular importance to users of existing computer codes and to developers of new calculation methods. For the problem at hand, a "computationally convenient" formula means a representation of the mean-velocity profile which has some or preferably all of the following characteristics: 1) it is a closed-form expression, 2) it gives u explicitly as a function of y , 3) it is valid over the whole width of the boundary layer, and 4) it is relatively easily evaluated. The objective of this Note is to provide such a formula for external boundary layers and pipe flows. The analysis holds for two-dimensional incompressible turbulent flow past a smooth surface but (being within the framework of the wall-wake similarity laws) fails in the cases of relaxing flows and flows characterized by the presence of very large positive or negative pressure gradients.¹

Coles² has shown that an expression of the form

$$u^+ = \frac{1}{\kappa} \ln y^+ + B + g\left(\Pi, \frac{y}{\delta}\right) \quad (1)$$

provides an accurate fit to experimental velocity data for both equilibrium and nonequilibrium turbulent boundary layers for $y^+ > 50$. However, in order to obtain velocity profiles valid over the whole width of the boundary layer one can write Eq. (1) in a slightly different way

$$u^+ = f(y^+) + g(\Pi, y/\delta) \quad (2)$$

where $f(y^+)$ is a representation of the law of the wall valid over the whole inner layer and is asymptotic at large y^+ to $(1/\kappa) \ln y^+ + B$. Function $g(\Pi, y/\delta)$ is a representation of the law of the wake. In Eqs. (1) and (2), Π is Coles' wake parameter.¹ For the function $g(\Pi, y/\delta)$ we adopt the expression

$$g\left(\Pi, \frac{y}{\delta}\right) = \frac{1}{\kappa} (1 + 6\Pi) \left(\frac{y}{\delta}\right)^2 - \frac{1}{\kappa} (1 + 4\Pi) \left(\frac{y}{\delta}\right)^3 \quad (3)$$

proposed independently by Finley et al.,³ Granville,⁴ and Dean.⁵ Equation (3) is an improvement over the more widely used form

$$g\left(\Pi, \frac{y}{\delta}\right) = \frac{\Pi}{\kappa} w\left(\frac{y}{\delta}\right) = \frac{2\Pi}{\kappa} \sin^2\left(\frac{\pi}{2} \frac{y}{\delta}\right) \quad (4)$$

since it describes more accurately the true boundary conditions on the wake function.⁴ In the present analysis it is assumed that in addition to u_e and ν the parameters u_τ , δ , and Π are known at the streamwise station in question. This is not a stringent requirement since any one of the five parameters u_τ , δ , Π , δ^* , θ can be determined if two of them are known.¹

Inner Layer (Law of the Wall)

A large variety of analytical representations of the law of the wall have been proposed, characterized by various levels of complexity and accuracy. Spalding's implicit formula may be considered the most widely used and is adopted by White⁶ and Dean⁵ as the accepted form of the law of the wall.

Spalding⁷ has shown that Laufer's experimental data⁸ for the mean velocity distribution in the inner layer are well fitted

by formulas of the form

$$y^+ = u^+ + e^{-\kappa B} \left[e^{\kappa u^+} - \sum_{n=0}^{\ell} \frac{(\kappa u^+)^n}{n!} \right] \quad (5)$$

where $\ell=3$ or 4 and κ and B are the parameters of the logarithmic law. Equation (5) satisfies (for $\ell=3$) or exceeds (for $\ell=4$) Reichardt's cubic power law for the eddy viscosity in the immediate neighborhood of the wall. Furthermore, it is asymptotic at large y^+ to the logarithmic law $u^+ = (1/\kappa) \ln y^+ + B$.

In what follows a very simple procedure of obtaining explicit analytical approximation of Eq. (5) is described. Then, a new formula is proposed which fits better the experimental data. The constants κ and B are taken as 0.41 and 5.0, respectively¹ throughout this work.

Assuming $\ell=3$ and differentiating Eq. (5) we obtain

$$\frac{dy^+}{du^+} = 1 + \kappa e^{-\kappa B} \left[e^{\kappa u^+} - 1 - (\kappa u^+) - \frac{(\kappa u^+)^2}{2} \right] \quad (6)$$

which by taking into account Eq. (5) can be written as

$$\frac{du^+}{dy^+} = \frac{1}{1 + \kappa \{ y^+ - u^+ + e^{-\kappa B} [(\kappa u^+)^3 / 6] \}} \quad (7)$$

Figure 1 shows a plot of du^+/dy^+ vs y^+ . This function can be accurately approximated over the infinite interval $[0, \infty]$ by a rational function of the form

$$R(y^+) = 1 - y^+ \frac{(y^+)^2 + a_1 y^+ + a_0}{(y^+)^3 + b_2 (y^+)^2 + b_1 y^+ + b_0} \quad (8)$$

which correctly emulates the asymptotic behavior of du^+/dy^+ provided that

$$b_2 - a_1 = 1/\kappa = 2.44 \quad (9)$$

Under this condition, the difference

$$e(y^+) = \frac{du^+}{dy^+} - R(y^+) \quad (10)$$

vanishes asymptotically as $y^+ \rightarrow \infty$. Moreover, the difference is zero at $y^+ = 0$. The value of the coefficients a_0, a_1, b_0, b_1, b_2 can be conveniently determined by imposing the condition $e(y^+) = 0$ at four points and Eq. (9). A series of numerical experiments have shown that a very good approximation of the function defined by relations (7) and (5) (for $\ell=3$) is achieved by imposing the condition $e(y^+) = 0$ at $y^+ = (2.0, 6.0, 10.0, 20.0)$. The corresponding values of the coefficients are: $a_0 = 6.0256$, $a_1 = -4.633$, $b_0 = 222.31$, $b_1 = 16.507$, $b_2 = -2.193$.[†] Analytical integration of Eq. (8) yields

$$u^+ = \ln \left[(y^+ + 4.67)^{2.24} (y^{+2} - 6.82y^+ + 48.05)^{0.101} \right] + 4.22 \tan^{-1} (0.166y^+ - 0.565) - 1.67 \quad (11)$$

which is in good agreement with Eq. (5). The relative difference is less than 0.8% for $1 < y^+ < 2$ and becomes significantly smaller for larger values of y^+ . The above technique has been applied to the case $\ell=4$. The resulting

[†]It should be noted that if a Remes-type algorithm is employed using the obtained approximation as initial guess it will converge to the best (in the Chebyshev sense) rational approximation.^{9,10} However, this is not necessary considering: 1) the very good approximation achieved by the simple interpolation procedure and 2) the nature of the approximated function (function generated by curve fitting of scattered experimental data).

approximation is

$$u^+ = \ln \left[\frac{(y^+ + 5.85)^{3.04}}{(y^{+2} - 9.25y^+ + 58.5)^{0.3}} \right] + 4.16 \tan^{-1} (0.164y^+ - 0.759) - 1.45 \quad (12)$$

The relative difference is less than 0.82% over the interval $[1, 2]$, being significantly smaller for larger arguments.

Plots of Eq. (5) for $\ell=3$ (curve I) and $\ell=4$ (curve II) are shown in Fig. 2 where comparison is made with the experimental data of Lindgren,¹¹ Perry,¹ Patel and Head,¹² and Durst.¹³ Spalding,⁷ based on Laufer's data,⁸ was unable to say which of the two curves gives the more precise fit. However, consideration of the experimental data shown in Fig. 2 indicates that curve I gives a better fit for $y^+ < 12$ and curve II shows better agreement for $y^+ > 20$. Thus, a function which closely follows curve I in the immediate neighborhood of the wall turns at $y^+ = 12$ and merges smoothly into curve II in the vicinity of $y^+ = 20$ describes better the data. Following the procedure described above one obtains the following representations of the law of the wall:

$$u^+ = \ln \left[\frac{(y^+ + 11)^{4.02}}{(y^{+2} - 7.37y^+ + 83.3)^{0.79}} \right] + 5.63 \tan^{-1} [0.12y^+ - 0.441] - 3.81 \quad (13)$$

The extent to which Eq. (13) fits the data can be judged by inspection of Fig. 2. It should be noted that Eq. (13) is based on no new physical assumptions and correlates data of nonuniform accuracy, obtained from experimental in-

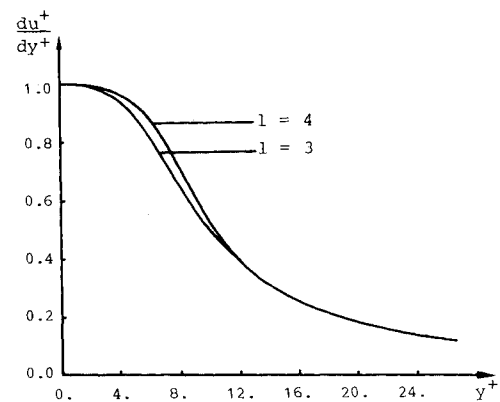


Fig. 1 Dimensionless velocity gradient according to Eqs. (7) and (5).

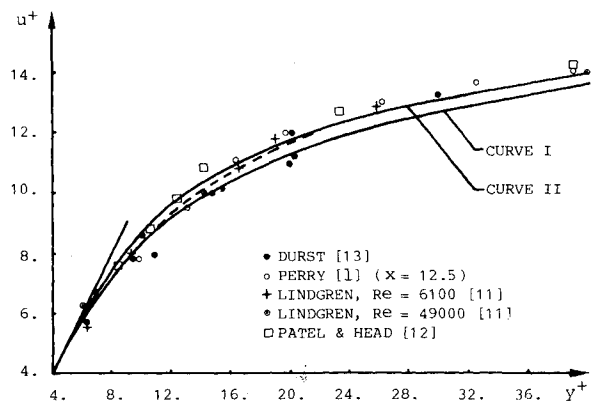


Fig. 2 Comparison of calculated and experimental velocity profiles in the buffer layer. Curve I: Eq. (5), $\ell=3$. Curve II: Eq. (5), $\ell=4$. ---: Eq. (13).

vestigations that have been carried out in different pieces of apparatus.

Conclusions

Any of Eqs. (11), (12), or (13) together with Eq. (3) give an explicit, closed form representation of the mean velocity profile in a turbulent boundary layer which is valid over the whole width of the boundary layer and fits well the experimental data. Equations (11) and (12) are accurate explicit approximations of Spalding's formulas for the law of the wall for $\ell=3$ and $\ell=4$, respectively; while Eq. (13) is a representation of the law of the wall which better fits the experimental data.

References

- ¹ Coles, D. E. and Hirst, E. A., eds., "Computation of Turbulent Boundary Layers," *Proceedings of the 1968 AFOSR-IFP-Stanford University Conference*, Compiled Data, Stanford University, Stanford, Calif., Vol. II, 1968.
- ² Coles, D. E., "The Law of the Wake in the Turbulent Boundary Layer," *Journal of Fluid Mechanics*, Vol. 1, July 1956, pp. 191-226.
- ³ Finley, P. J., Khoo, C. P., and Chin J. P., "Velocity Measurements in a Thin Turbulent Water Layer," *La Houille Blanche*, Vol. 21, 1966, pp. 713-721.
- ⁴ Bradshaw, P. (ed.), *Turbulence*, 2nd Ed., Springer-Verlag, Berlin, 1978, p. 136.
- ⁵ Dean, R.B., "A Single Formula for the Complete Velocity Profile in a Turbulent Boundary Layer," *Journal of Fluids Engineering*, Vol. 98, Dec. 1976, pp. 723-726.
- ⁶ White, F.M., *Viscous Fluid Flow*, 1st Ed., McGraw-Hill, New York, 1974, pp. 474-477.
- ⁷ Spalding, D.B., "A Single Formula for the Law of the Wall," *Journal of Applied Mechanics, Transactions of ASME, Series E*, Vol. 83, Sept. 1961, pp. 455-458.
- ⁸ Laufer, J., "The Structure of Turbulence in Fully-Developed Pipe Flow," NACA Report 1174, 1954 (supersedes TN 2954).
- ⁹ Cody, W.J., Fraser, W., and Hart, J.F., "Rational Chebyshev Approximation Using Linear Equations," *Numerische Mathematik*, Vol. 12, 1968, pp. 242-251.
- ¹⁰ Meinardus, G., *Approximation of Functions: Theory and Numerical Methods*, Springer-Verlag, Berlin, 1967, Chap. 9.
- ¹¹ Lindgren, E. R., "Experimental Study on Turbulent Pipe Flows of Distilled Water," Dept. of Civil Engineering, Oklahoma State Univ., Rept. 2, July 1965.
- ¹² Patel, V. C. and Head, M. R., "Some Observations on Skin Friction and Velocity Profiles in Fully Developed Pipe and Channel Flows," *Journal of Fluid Mechanics*, Vol. 38, Aug. 1969, pp. 181-201.
- ¹³ Durst, F. and Rastogi, A. K., "Calculation of Turbulent Boundary Layer Flows with Drag Reducing Polymer Additives," *Physics of Fluids*, Vol. 20, Dec. 1977, pp. 1975-1985.

Turbulent Nonreacting Swirling Flows

J. I. Ramos*

Carnegie-Mellon University, Pittsburgh, Pennsylvania

Introduction

THE purpose of this work is to present some numerical results for incompressible, confined, swirling flows in a model combustor. These results have been obtained by means of the $k-\epsilon$ and $k-\ell$ models of turbulence^{1,2} and compared with

the experimental data of Vu and Gouldin.³ The calculations have been performed in a model combustor which consists of a 3.43 cm diam inner pipe and a 14.5 cm diam outer pipe. The outside diameter of the inner pipe is 3.86 cm. The turbulence models used in this study use an isotropic eddy diffusivity whose validity in swirling flows has been seriously questioned, e.g., Ref. 4. The models solve the axisymmetric form of the conservation equations of mass; axial, radial, and tangential momentum; turbulent kinetic energy k ; turbulent length scale ℓ ; or dissipation rate of turbulent kinetic energy ϵ . Similar calculations have been performed by Srinivasan and Mongia,⁵ who employed the $k-\epsilon$ model and who also compared their theoretical results with the experimental data of Vu and Gouldin.³ Srinivasan and Mongia⁵ concluded that the $k-\epsilon$ model had to be modified to include the effects of the curvature Richardson number in order to predict a recirculation zone for both coswirl (jets rotating in the same direction) and counterswirl (jets rotating in opposite directions) conditions. In this Note, however, it is shown that the $k-\epsilon$ model does predict a recirculation zone for both co- and counterswirl flow conditions if suitable inlet conditions are used. The effect of the inlet conditions on the flowfield has been previously investigated by Ramos,^{1,2} and Abujelala and Lilley.⁶ The latter showed that small changes in the inlet conditions produce drastic changes in the flowfield.

Presentation and Discussion of Results

Some representative results obtained with the $k-\epsilon$ and $k-\ell$ models are shown in Figs. 1 and 2. These figures present the mean axial and mean tangential velocity profiles along the combustor, i.e., at different values of z/R_i where z is the distance from the inner pipe exit and R_i is the inner pipe radius, as a function of the normalized radial distance. In these figures, the axial u and tangential w velocity profiles have been normalized by the inner jet inlet velocity which is uniform. The figures correspond to the cases A-D studied by Vu and Gouldin³; these cases are reproduced in Table 1. In this table, α denotes the outer-to-inner-jet inlet velocity ratio, and S_i and S_o denote the inner and outer swirl numbers.

In Figs. 1 and 2, the dots correspond to the experimental values of Vu and Gouldin.³ However, since these investigators did not obtain fully axisymmetric flows, the data in these figures correspond to the average of the experimental values on both sides of the combustor symmetry axis. The solid and dotted lines in the figures correspond to the numerical results obtained with the $k-\ell$ and $k-\epsilon$ models. Figure 1 shows the mean axial velocity profiles for cases A and B,

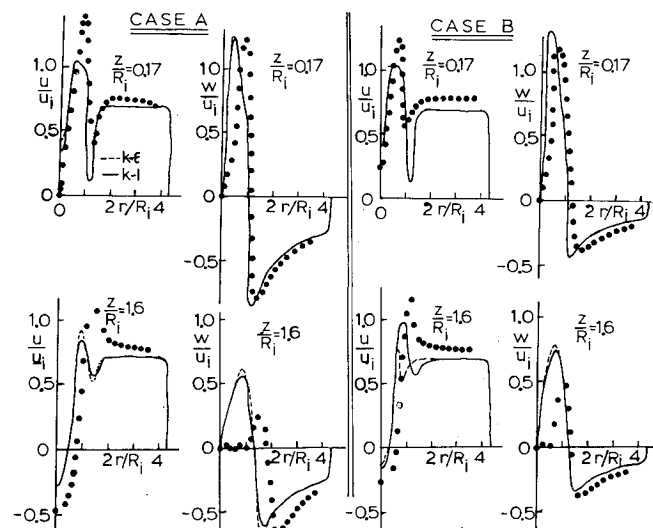


Fig. 1 Mean axial and tangential velocity profiles. Conditions A (left) and B (right).

Received Feb. 15, 1983; revision received Aug. 5, 1983. Copyright © American Institute of Aeronautics and Astronautics, Inc., 1983. All rights reserved.

*Assistant Professor, Department of Mechanical Engineering. Member AIAA.